AIAA-96-0851

Review of Optical Diagnostics for Hypersonic Low-Noise Ludweig Tube Facilities

S. H. Collicott, S. P. Schneider,
N. L. Messersmith
School of Aeronautics and Astronautics
Purdue University
West Lafayette, IN 47907-1282

34th Aerospace Sciences Meeting & Exhibit
January 15-18, 1996 / Reno, NV

REVIEW OF OPTICAL DIAGNOSTIC METHODS FOR HYPERSONIC LOW-NOISE FACILITIES

Steven H. Collicott*, Steven P. Schneider† and Nathan L. Messersmith‡
Purdue University
West Lafayette, IN 47907-1282

Abstract

Research in hypersonic boundary layer receptivity and transition on aerodynamic bodies requires the use of low-noise (quiet-flow) facilities. The thermodynamic and aerodynamic states of the test-section flow in low-noise facilities imposes unique requirements on optical diagnostics methods. A discussion of these requirements is presented, followed by the measurement requirements for hypersonic boundary layer transition research, and the evaluation of a number of intrusive and optical diagnostic methods. The laser differential interferometer is found to be the best candidate for acquiring high-bandwidth ($> 1\,\mathrm{MHz}$) data within the boundary layer ($\delta \leq 1\,\mathrm{mm}$).

Introduction

Reliable prediction and control of high-speed laminar-turbulent transition on realistic flight vehicles requires continued experimental research. Interpretation of most existing transition data is ambiguous due in large part to the scarcity of measurements documenting the mechanisms leading to transition. Measurements of the small-amplitude 3-d instability waves that lead to transition have only been carried out using hot wires, which are intrusive, fragile, and often have insufficient bandwidth for unsteady high-speed flows. To overcome these difficulties and to complement the hot-wire measurements the application of optical diagnostic methods is desirable.

It is shown that the flow characteristics unique to quiet-flow hypersonic facilities[1] present rigorous requirements that few optical diagnostics methods can meet. This review is not exhaustive; variations on optical methods seem to be continually invented or rediscoverd. Review efforts to date, which continue as a constant effort to find the best manner to unlock the secrets of hypersonic boundary layer transition, show that one optical method stands out as most practical. The Laser Differential Interferometer[2, 3, 4], or LDI for short, appears to best meet requirements. Although the probe volume is long in one dimension, compared to typical displacement thicknesses of 1 mm, careful experimental design should allow for quantitative comparisons to theory. Resolution of minute optical path-length differences of 0.0013 wavelengths with a signal-to-noise ratio (SNR) of 150 has been demonstrated by previous workers. This performance should make possible highly-resolved measurements of 1% density fluctuations in a Mach 4 boundary layer with an edge density 4% of that at room temperature and pressure. High sensitivity, high bandwidth, nonintrusive measurements of Mach 4 boundary layer transition appear to be feasible in a low-noise facility only with this technique.

Outer Flow Conditions

The Purdue University Quiet-Flow Ludweig Tube (Figure 1) has been in operation since January, 1994[1]. Root-mean-square total pressure fluctuations in the quiet-flow test core are consistently below 0.1% for $P_o \approx 1$ atm, and $T_o \approx 295\,\mathrm{K}$. Isentropic expansion to Mach 4, with negligible total pressure drop through the unsteady expansion process, creates the free-stream conditions in Table 1. As a simplified example of the class of aerodynamics geometries of interest (presently 4:1 elliptic cones), a 5 degree circular cone flow is solved to estimate edge conditions for the boundary layers. These quantities are also presented in Table 1.

Scales and Resolution

Boundary layer computations have been carried out for these parameters, using a two-dimensional finite difference code [5]. A surface temperature of 295 K would be typical, for the model temperature can be assumed isothermal due to the short run-time. The displacement thickness, δ^*, 100 mm from the leading edge is 0.7 mm, while the 99.5% thickness is 1.0 mm. The inviscid surface velocity is about $670\,\mathrm{m\ s^{-1}}$. Thus, the boundary-layer turnover time, U_e/δ^*, is about 1.0 MHz.

*Assistant Professor, School of Aeronautics and Astronautics. Senior member, AIAA
†Associate Professor, School of Aeronautics and Astronautics. Member, AIAA
‡Assistant Professor, School of Aeronautics and Astronautics. Member, AIAA

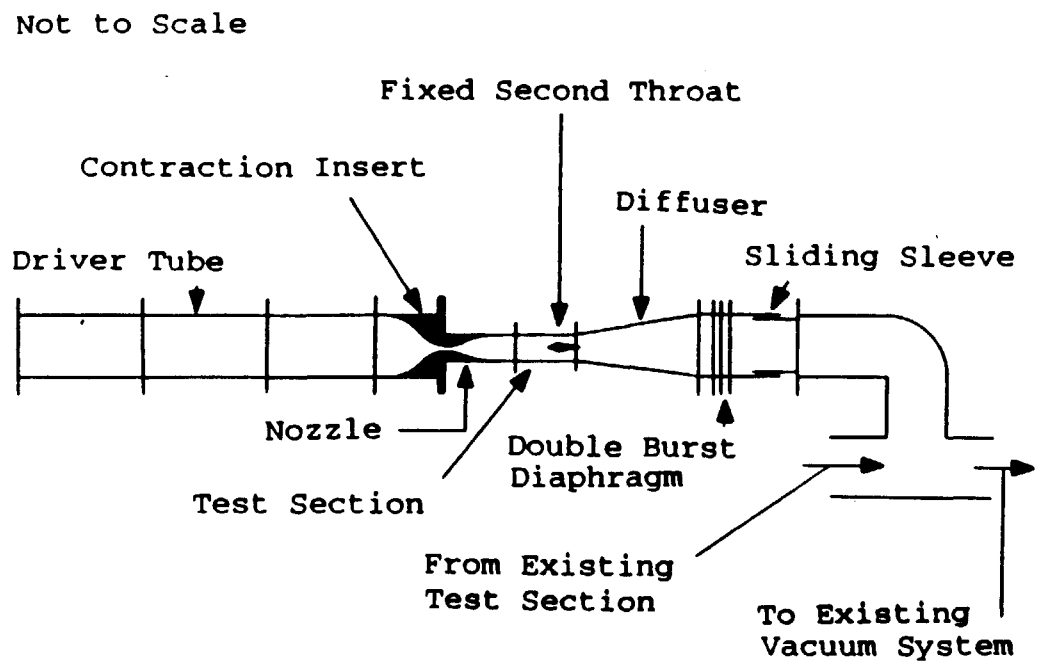

Figure 1: Schematic of the Purdue Quiet-Flow Ludwieg Tube. The test section Mach number is 4.0, and the run time is approximately 3 seconds. Test section size is nominally 4 in square.

The instability waves that form the mechanisms of transition in these flows fall into several categories. The first and second mode TS-like waves have been reviewed by Mack [6]. One of the few references that gives details of the fluctuation profiles was carried out for similar conditions, at Mach 4.5 on a hollow cylinder model [7]. At a Reynolds number based on displacement thickness of 10^4, both the first and second mode instability waves were computed. The wavefronts of the first-mode instability, which are always oblique at high speed, have an angle of 58 degrees with respect to the streamwise direction, a wavelength of $13\delta^*$, and a frequency $f = 0.06U_e/\delta^*$. We can thus estimate that first-mode waves observed on the elliptic cone will have wavelengths of roughly 5-15 mm , frequencies of roughly 30-90 kHz, and wave angles of perhaps 50-70 degrees. It should be noted that Pruett et al observed that $\delta^* \simeq 10\sqrt{x\nu_e/U_e}$ at Mach 4.5, for a range of conditions. Fluctuations profiles for the first-mode waves are shown in Fig. 2, taken from [7] (see also [8]).

The amplitudes of the fluctuations in this figure are normalized by the mean value of the quantity at the edge of the boundary layer. Temperature fluctuations dominate the disturbance, and the peak in these fluctuations is in the outer half of the boundary layer, about $1.1\delta^*$ from the wall. Density fluctuations are next-largest, about 40% of the amplitude of the temperature fluctuations, and peak about $1.2\delta^*$ from the wall. Velocity fluctuations are much smaller, about 10% of the temperature fluctuations, and peak about $1.0\delta^*$ from the wall. Pruett et al show that secondary instabilities become significant when the temperature fluctuations are 1-3% of the edge temperature, for both first and second mode waves. This observation is in general agreement with experimental experience that 1% fluctuations are large waves that will soon transition to turbulence. For a large first-mode instability wave of 1% amplitude, T' peaks at about 1 K, ρ' at roughly 0.15 gm m^{-3}, and u' at roughly 0.7 m s^{-1}. All three of these fluctuation peaks are in the outer part of the boundary layer.

Second-mode instability waves are also observed by Pruett et al at the same location. These have a wavelength of about $2.8\delta^*$, a frequency of about $0.3U_e/\delta^*$, and wavefronts normal to the streamwise direction. We can thus estimate that second-mode waves in our facility would have wavelengths of about 2 mm , frequencies of about 300 kHz, and will be spanwise uniform. Fluctuation profiles for these waves are shown in Fig. 2, also taken from Pruett[7]. Again, temperature fluctuations dominate the disturbances, with

	Density ρ, kg m^{-3}	Pressure P, kPa	Temperature T, K	Enthalpy h, J kg^{-1}	Velocity V, m s^{-1}
Total	1.2	101	295	3.0×10^5	0
Free stream	0.033	0.67	70	0.71×10^5	670
Approximate:					
Edge	0.039	0.85	75	0.78×10^5	664
Surface	0.010	0.85	295	2.9×10^5	0

Table 1: Approximate flow quantities for a 5 degree cone in the Purdue University Mach 4 Quiet-Flow Ludweig Tube

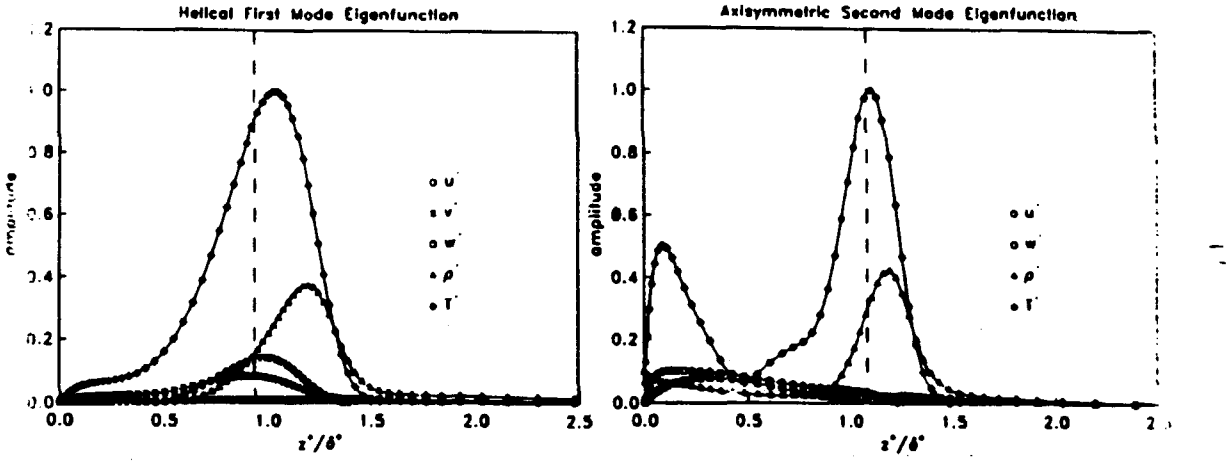

Figure 2: Fluctuation Profiles for Typical First-Mode (left) and Second-Mode (right) Instability Waves. Figure is from Pruett[7].

an amplitude that peaks at about $1.1\delta^*$; a secondary peak of about half the primary amplitude is also present near the wall. Density fluctuations are again about 40% of the temperature fluctuations, and again peak at about $1.2\delta^*$, without any secondary peak near the wall. Velocity fluctuations are less than 10% of the temperature fluctuations, and are largest in the inner half of the boundary layer. The general amplitude of these fluctuations is about the same as for first-mode waves, except the u' fluctuations are about half as big and nearer the wall, and the T' fluctuations also have a secondary peak near the wall. The major differences between first and second-mode waves lie in the frequencies and wavelengths, which differ by a factor of about 5.

Finally, a discussion of the requirements for resolving the intermittent region of transition is required. Typical frequencies inside the turbulent spots that make up this region are of the order of the boundary-layer turnover frequency, 1 MHz. Resolving the leading and trailing edges of the spots to within $1\delta^*$ will also require 1 MHz bandwidth, since the spots convect at nearly the free stream velocity.

These estimates are of necessity rough, due to the lack of detailed computations for complex configurations, yet they demonstrate the level of resolution required for characterization of transition mechanisms in low-noise hypersonic facilities. High sensitivity is required to measure small fluctuations that are an order-of-magnitude smaller than those typical of turbulence. High-bandwidth continuous-time data is

also required, so that the characteristic frequencies of the disturbances can be determined. Since second and higher harmonics of the disturbances can be significant near transition, bandwidths of 1 MHz are highly desirable.

Requirements for Comparison to Theory

Theory and numerical computation have progressed to the level where detailed quantitative comparisons are required in order to determine the direction of future theoretical developments. For example, integrated e^N computations are currently carried out in several forms: 1) disturbances that vary in frequency and 3D shape as they travel downstream in order to always achieve the highest local growth rate, 2) disturbances that maintain the same frequency and 3D shape as they travel, 3) disturbances that travel along group velocity trajectories in 3D flows, 4) disturbances that travel along the local inviscid streamline in 3D flows. Detailed measurement of the 3D unsteady wave field is required to address these issues. This is non-trivial, even for measurements phase-referenced to controlled perturbations.

Evaluation of theoretical assumptions and numerical methods, and also exploratory investigations of new phenomena, require unambiguous measurements that can be directly compared to theory. Since information on the entire 3-D unsteady flow field is becoming fairly straightforward to compute, any well-defined derived quantity can be computed. Thus, the differential density fluctuations integrated through small probe volumes that will be produced by the LDI are quantities easily computible from 3-D unsteady CFD results.

Background: Intrusive Techniques

Hot-Wire and Hot-Film Anemometry

Hot wire anemometry is certainly the dominant technique for the measurement of transition mechanisms at high speed. Measurements of instability waves using hot wires have been carried out by Demetriades (e.g., [9]), Kendall (e.g., [10]), and Stetson (e.g., [8]), to name the principal contributors. Most workers use constant-current methods along with traditional mode diagrams, although constant-temperature methods can also be used [11, 12]. Calibrations of the hot wire voltage versus mass-flux can readily be performed for constant-temperature wires operated at high overheats. Constant-current operation at a variety of overheats allows separation of the mass-flux and total-temperature fluctuations. Of course, the signal must remain stable while the overheat is being varied, which is not a trivial task.

Bandwidth of 300-400kHz can be observed in careful practice. The considerable pains taken at AEDC for Stetson's work resulted in a bandwidth of about 600 kHz. The spatial resolution in these measurements is closely related to the wire size, which was 0.5 microns in diameter and 0.1 mm in length. Mass-flux fluctuations of 0.1% were readily measured, along with stagnation-temperature fluctuations of 0.01%. These high sensitivities are obtained using careful amplification and signal processing. Operation of an anemometer at multiple overheats during a short-duration run has already been demonstrated by Walker [13], showing that use of the classical mode-diagram approach in constant-current operation is also practical.

However, hot wires are intrusive, delicate, require calibration, and have a limited frequency response. Operation with multiple wires becomes very difficult due to the blockage of the traverse systems required to hold the wires. Wires cannot be located downstream of each other, for the same reason. Although the delicacy of the wires is alleviated by the particle filtering which is already required for quiet flow, the wires fail fairly often and repair is not easy. Wires cannot be readily positioned in some parts of the flow (near the nose of a blunt body, say), due to geometrical constraints. The application of optical techniques to complement hot wire anemometry is clearly necessary.

Surface-mounted hot films have also been used for measurement of transition mechanisms and intermittency, for example, [14] and [15]. Although most such uses have been at low speeds, a few workers have successfully studied high-speed flows. Owen[16] reported use of hot-films for detection of transition on flat plates at speeds to Mach 4. However, Owen does not report any intermittency data, nor does he display time-traces showing the passage of turbulent spots. The technique is limited by (1) the limited frequency response of hot-films, and (2) the movement of the transitional disturbances to the outer part of the boundary layer with increasing Mach number. The limited frequency response of the sensors was explored by the second author using shock-tube tests of custom-built sensors as small as 12 μm by 125 μm [17, 18]. The highest frequency response that could be obtained was about 110 kHz, which falls well short of the 1 MHz frequencies characteristic of the Mach 4 boundary layers to be studied. Turbulent fluctuations with frequencies to 60 kHz have been measured in a Mach 3 boundary layer on a flared cone by the second author, but only with limited signal-to-noise ratio [19]. The frequency response of surface thin-films operated in heat-transfer sensing mode is also

limited to about 100 kHz [20]. However, Clark et al. [20] have mapped the path of turbulent spots at Mach 0.55 using arrays of surface-mounted hot-films, and Schmisseur et al. [21] present results extending the hot-film technique to our Mach 4 Ludwieg tube. Although the full frequency content of the turbulence is not captured, and only the surface footprint of the turbulent area is measured, it nevertheless appears feasible to map out the surface footprint of the turbulent regions in the intermittent flow. Because of (2) above, however, it does not appear feasible to use surface-mounted hot films to measure the high-speed instability waves themselves. Finally, although deposition of hot-film arrays on flat Kapton sheets is relatively inexpensive, and effective for developable surfaces with curvature in one direction, multiply curved surfaces will be more difficult, for the flat Kapton sheets on which the films are normally deposited will not deform so as to adhere smoothly to a surface with curvature in two directions. Thus, the number of realistic geometries that can be investigated may be limited.

Background: Optical Methods

Optical methods appear to fall into three categories: interaction with particles, interaction with molecules or atoms, and transmitted wave techniques.

Scattering for Optical Diagnostics

Many instruments must use light scattered from particles in the flow because the light scattered from molecules is typically much weaker, and is also temperature-broadened. The use of particulates in quiet-flow nozzles is particularly sensitive, since particles above 1 μm in diameter must be filtered out to preclude particles tripping early transition on the nozzle walls. Fortunately, a large number of particles are condensed out in high-speed flows due to the large temperature reductions in the free stream. At Mach 4 and the operating conditions in our facility, nitrogen and oxygen do not condense, but water vapor and carbon dioxide do (see [22] for an excellent review). The maximum level of these condensates is limited by the acceptable amount of flow deviation caused by the heat released when the vapor condenses to solid crystals. Figure 76 from Reference [22] shows that a mass fraction of 0.05 gm water vapor per kg of air is the maximum amount that will not cause static pressure variations larger than 0.5% in a typical test. Allowing for a factor of 10 increase above this, to be generous in scattering estimates, assume 0.5 gm of water vapor per kg of air. This level is approximately matched by the normal carbon dioxide content of the air.

At a typical test-section static pressure for our facility, 0.1 psi, water vapor condenses at 193 K and carbon dioxide at 107 K. Since the free stream static temperature is 71 K, both of these species will normally condense by the time the flow enters the test section[23]. Assuming that the density of the condensed phase is approximately equal to that of liquid water, the volume fraction of condensed water is 1.7×10^{-9}, and of carbon dioxide is 9.5×10^{-9}. The size of the particles that condense is determined by the rate of cooling experienced by the air, among other factors, so that the particle size is nozzle-dependent. However, particle sizes reported from light-scattering measurements are in the range of 200-600 nm [23] for water vapor. If we assume a typical particle size of 300 nm , the above volume fractions correspond to 15,000 water drops per cubic mm, and 84,000 carbon dioxide drops per cubic mm. Only 15 water drops will then be contained in a cube of sides 0.1 mm , a probe volume that is a suitably small fraction of the boundary-layer dimensions.

Since these particles are extremely small, they should remain in equilibrium with the local gas, once they are condensed out [22]. This makes the carbon dioxide particles not very useful for boundary-layer work on adiabatic-wall models, since they will return to vapor at $T/T_e \simeq 1.5$, which corresponds only to the part of the boundary layer outside one displacement thickness. However, the water vapor particles are likely to be useful for high-speed work, since they will not return to vapor until they reach $T/T_e \simeq 2.7$. This location corresponds to about $0.8\delta^*$ from the wall, which is sufficient to allow capturing most of the fluctuation peaks described in the section on the flow physics. Of course, the path taken by the boundary-layer gas becomes critical if these particles are to be used. For example, if the particles travel through a stagnation region, they will probably remain in the vapor state, partially supercooled, as they travel downstream. Cold-wall studies would allow the particles to remain in the condensed phase nearer the wall, but even in a cold-wall boundary layer a large region of viscous-heated gas exists in the middle region away from the wall.

Typographical errors in [23] preclude reconciliation of their data with these dewpoint-based estimates, yet these figures should form a useful order-of-magnitude estimate for the number of scatterers to be expected. Although larger numbers of scatterers can be obtained if the average size decreases, the volume fraction limit corresponds to the mass-fraction loading of the two condensing species. Although un-

certainties in the density of the condensed phase and in the particle size are large, we expect that these estimates are probably accurate within a factor of 100 or so. Higher volume fractions can be allowed, perhaps, for turbulence work, and other measurements insensitive to perturbations, but are unlikely to be permissible for measurements of transition mechanisms.

Calculations of particulate scattering[24] in desirably-sized sample volumes (0.01 cm on a side) in our flow indicate that F/2 collection optics will collect approximately 10^{-13} of the incident light (wavelength of 0.5 μm). In contrast, Rayleigh scattering from the nitrogen molecules is a substantially weaker process per scatterer, but there are far more molecules than condensed scatterers per unit volume. Based on the flow described in Table 1, the number density of nitrogen molecules at the edge of the boundary layer is $n = 8.6 \times 10^{17}\,\mathrm{cm}^{-3}$. Assuming a Rayleigh scattering cross section[25] of $\sigma = 4 \times 10^{-28}\,\mathrm{cm}^{2}\,\mathrm{sr}^{-1}$, a desired measurement volume 0.01 cm on a side, and F/2 collection optics gives a collection efficiency of approximately 10^{-13}. It is both coincidental and unfortunate that this is the same order of magnitude as the condensed particulate scattering described above.

Thus, for either molecular or particulate scattering, a 1 Watt (or Joule) laser would produce 10^{-13} Watts (or Joules) on a detector. This power translates to about 3×10^{5} photons per second, which is only 0.3 photons per microsecond arriving on a detector, such as a photo-multiplier tube (PMT). Thus, a 10 Watt continuous laser would be sufficient for measuring the mean flow, but not 1 MHz fluctuations. Bear in mind that shot noise in the detection process is equal to the square root of the mean[26], so 1% resolution within a sampling interval (1 μs for the 1 MHz bandwidth) requires at least 10^{4} photons during that interval, or a 3 kW laser.

If one considers a short-pulsed laser, such as a Q-switched Nd:YAG, the 3×10^{5} photons are sufficient for detection by photomultiplier tubes or intensified electronic cameras. However, at these weak scattering conditions, the proximity of the model surface to the measurement volume is prohibitively troublesome[27], and more the elaborate methods discussed below must be considered.

Optical Velocimetry Methods

Numerous optical instruments useful in other flows are found not to be feasible in our flow. Laser Doppler Velocimetry (LDV), Particle image velocimetry[28] (PIV) (or a variant, laser speckle velocimetry[28] (LSV)), and Doppler global velocimetry[29] (DGV), and the laser interference velocimetry[30, 31] (LIV) rely on scattering of light from particles in the flow. Filtered Rayleigh scattering[32] (FRS) collects light scattered from molecules. LIV uses on a continuous laser source, FRS and PIV/LSV in this velocity range use a short-pulsed source, and variants of DGV can be made with either pulsed or continuous sources. Several systems that may be suitable for mean flow measurements fail when applied to trying to measure these small amplitude, high-frequency waves in density, temperature, and velocity within the boundary layer. Investigation of the mechanisms of transition, and not measurement of the mean flow field, is the goal of research in quiet-flow facilities.

PIV/LSV

PIV and LSV measure velocities as particle displacements between exposures (laser pulses). Thus, the distance a particle or group of particles moves between exposures sets the minimal length scale for spatial resolution of velocities in both PIV[33] and LSV[34]. Similar to LDV, velocity gradients within the interrogation region cause a bias in, and averaging of, the velocities within that region, plus a decrease in SNR. Velocity difference top-to-bottom in a 0.1 mm diameter region of the boundary layer would be on the order of $(U_e/\delta) * 0.1\,\mathrm{mm}$. This is approximately 70 m s $^{-1}$ in our flow. The 1% of U_e fluctuations being sought are on the order of 7 m s $^{-1}$. Thus our goal would be to resolve 1% fluctuations within a region where the mean flow varies by 10%. Recent work by the leaders in PIV has led to slightly better than 1% resolution[28, 35], though not with the large velocity gradients expected within a single measurementcell of teh double-exposure. LSV has been shown to produce a smaller signal-to-noise ratio than PIV[34], so at best comparable uncertainty could be achieved. With the conflicts in velocity scales, the lack of demonstrated sub-percent resolution, and poor scattering performance (molecular scattering comparable to particulate scattering), PIV/LSV is not feasible for measuring the small fluctuations, and perhaps not even for mean-flow measurements.

Laser Doppler Velocimetry (LDV)

With photons arriving at a detector at a rate of approximately 1 MHz, it is not possible to have a heterodyne detection system for a typical LDV beat frequency on the order of 10 to 100 MHz[26]. Enlarging the sample volume helps this somewhat, but not nearly enough to make it practical. Similar velocity gradient and bias effects as discussed in the PIV/LSV section above would plague the measurements. Thus, the extremely weak scattering and large velocity gradients renders LDV impractical in our flow.

Doppler Global Velocimetry (DGV)

Weak scattering and uncertainties of the achievable resolution in velocity lead us to consider Doppler global velocimetry not to be feasible for our experi-

ments. Even with good strong scattering, achieving an uncertainty less than 1% amidst temperature and density fluctuations appears difficult to achieve with measurements made from ratios of digitized intensities. Similar to LDV and PIV, the range of velocities between the top and bottom of the measurement volume will be an order of magnitude greater than the fluctuations. Add to this the uncertainty of particle vaporization within the boundary layer, and we do not see DGV as a practical choice for measuring fluctuations in the boundary layers in our experiments.

Laser Interference Velocimetry (LIV)

Laser interference velocimetry[30, 31] (LIV) has several desirable qualities. The signal is continuous, 1 MHz bandwidth is possible, the measurement volume may be small, and it is non-intrusive. The drawback is that to achieve a sufficiently high signal-to-noise ratio for our work, approximately 0.1 μW of scattered power is required[31]. With our condensed scatterers described above, use of LIV in our experiment would require a 10^6 Watt laser, which is clearly impractical and likely intrusive.

Density-based Optical Methods

Filtered Rayleigh Scattering (FRS)

The basic concept of filtered Rayleigh scattering involves the use of an atomic or molecular absorption line to filter the scattered light[36, 32]. In this way, suppression of spurious scattering enables weakly scattered light to be resolved near a surface. Typically iodine vapor is used as the filtering gas. The nature of the filter can be adjusted by modifying the pressure and temperature of the iodine, but limiting conditions exist. For example, filter edges cannot be made infinitely steep and the minimum filter bandwidth is restricted. These effects all serve to reduce the accuracy of FRS.

In the elliptical cone boundary layer flow field a pulsed laser is necessary for FRS. As discussed above, roughly 10^6 photons from a 1 Joule laser pulse will be collected onto the detector. Collection must be perpendicular to the light sheet to obtain the best spatial resolution. In this case, though, the signal is a function of velocity, temperature and density. For perpendicular imaging, the mean flow Doppler shift is 70% of the maximum possible shift, which may amount to frequency shifts on the order of 1 GHz or more for high speed flows. Velocity fluctuations of 0.1% translate to roughly 1 MHz fluctuations in frequency, which are not measurable when superimposed over the scattered spectral width of 1 to 2 GHz (for the low temperature of the Mach 4 flow). The influence of temperature and density fluctuations are estimated with detailed modeling of both the scattering physics (using kinetic theory[37, 38]) and the iodine absorption processes in the filter cell. For a 1% fluctuation in temperature from the wind tunnel baseline conditions, calculations reveal that the change in the scattered signal will vary by approximately only 1 part in 10^6 from the baseline signal. Unfortunately, this is ± 1 photon at the estimated signal level from our flow.

Lastly, the Doppler shifts as mentioned above will bring the scattered spectra into a region of interaction with neighboring iodine absorption lines. The presence of these lines removes linearity in the signal analysis, requiring sophisticated quantum mechanical modeling of the absorption cell and detailed kinetic theory modeling of the scattering process to deconvolve the transmitted signal. At best, these models may be accurate to within a few percent at low pressures[37, 38]. As illustrated with the above examples, filtered Rayleigh scattering will not permit highly sensitive measurements of small amplitude fluctuations in high speed boundary layer transition.

An interesting two-color Rayleigh scattering method[25] unfortunately also suffers from some surface scattering. In a continuous mode, it too is rendered impractical by our weak scatterers. In a Nd:YAG laser method, our estimates show that it is not feasible to remove effects of surface scattering sufficiently well to come close to the necessary density or temperature resolution.

Shadowgraph, Schlieren, Interferometry

All four of these methods make use of the deformation of optical waves transmitted through a flow to visualize or record flow structures. High-speed shadowgraph or schlieren have been considered for this experimental program. They remain as candidates for visualizing some flow structures (shocks, thick turbulent boundary layers), but are unlikely to be able to resolve the small density variations contained in the instability waves. Both schlieren and shadowgraph methods rely on the refraction of rays by a spatially-varying density field. Unfortunately, the edges of the wind tunnel model diffract light, which, when cut by the aperture stop of the imaging system, often produces "ringing" in the images. This effect is often enhanced by the presence of the knife edge in schlieren systems. Sensitivity and spatial resolution compete in the design of these systems. Based on our experience in using shadowgraph for detecting conical bow shocks during our tunnel-starting tests, we can not have confidence that the minute index of refraction variations in the density waves would be both detectable and sufficiently spatially-resolved.

Interferometry, and holographic methods such a double-exposure holographic interferometry, are well-established techniques. To briefly explain their shortcomings for this application, consider that a shift of one fringe in the interferogram corresponds to 1 wave of phase delay in the signal beam. As explained above, our signal beam will likely contain only 0.001 waves of phase delay. Consistent with Smeets's substantial review of interferometric methods for wind-tunnel use[2], we conclude that the classical fringe-pattern type of interferometer falls far short of the required sensitivity.

Laser Differential Interferometry

Fig. 3 (from Smeets's Fig. 46[2]) shows a basic laser differential interferometer with an electro-optic phase modulator controlled by a feedback signal, derived from the PMT outputs, for stabilization or to maintain optimal sensitivity. This is fundamentally the same differential interferometer as Azzazy et al[3] and Smeets used, with small changes to better fit our flow facility and to provide versatility. The fundamental principle of operation is that the difference in phase between the wavefronts of the two beams determines the signals at the two photomultipliers. Any phase disturbances experienced by both beams, such as vibrations of a mirror mount, do not affect the differential phase. Complete details of operation may be found in reports by zAzzazy et al[3], or Smeets[2].

What makes this interferometer useful in the boundary layer studies is that the high frequencies characteristic of the boundary layer instability waves are not present in the outer flow. Thus when the two beams are interfered, the effects of the room air, bow shock, window bulging, outer flow, and similar are effectively nulled out, and only the phase differences acquired during passage through the boundary layer remain. Hence it is essential to consider the magnitudes of the densities and optical phase differences present in our experiments. The boundary-layer edge density at Mach 4 flow around a 5-degree cone in our tunnel is approximately $\rho_e = 0.04\,\mathrm{kg\ m^{-3}}$. This results in an index of refraction $n_e \approx 1.00001$. A 1% density fluctuation will cause a change in index of $\Delta n = \pm 10^{-7}$. Thus a distance of 10^7 wavelengths is required to build up a 2π phase difference. 10^7 waves of 488 nm light is nearly 5 m . Therefore, to detect the phase change acquired over a representative 1 cm path length through the boundary layer, the ability to detect a phase delay of approximately 0.002 waves is required. Because of the extremely small phase differences characteristic of our receptivity experiments, a fringe-pattern type of interferometer is not practical.

Fortunately, detection of 10^{-5} waves of phase delay has already been demonstrated by Smeets[2] with this type of boundary-layer interferometer. Additionally, Azzazy et al[3] have *independently* demonstrated a SNR of 150 for measurement of 0.0013 waves of phase delay in a similar system. Thus we are confident that this differential interferometer with feedback is a suitable instrument for our instability wave studies. It is worth noting that such a highly sensitive instrument is ultimately most useful in a quiet flow tunnel with good optical access like the Purdue Mach 4 facility[1].

Conclusions

When performed in quiet-flow facilities[39, 40], experiments on hypersonic boundary layer transition possess characteristics which preclude the use of a large number of common optical measurement and visualization techniques. Even if a technique is applicable as a mean flow diagnostic, the boundary layer research which requires use of quiet-flow facilities adds additional constraints which render many techniques unsuitable. The principle detriments to optical diagnostics are low mass density in the test section, and low molecular and particulate scattering efficiencies.

The one optical technique that stands out as an applicable boundary layer optical diagnostic tool is the Laser Differential Interferometer[2, 3, 4]. The benefits of such a non-intrusive instrument are a sufficiently small sample volume, continuous-time signal with high bandwidth, and high sensitivity. All this is achieved with a pleasantly simple apparatus.

Future low-noise hypersonic facilities are expected to produce similar low density in the test section, albeit with warmer flow that rules out hope for use of condensed scatterers while maintaining the same prohibition against passing solid particles through the throat. The warmer flow also increases the thermal broadening of Rayleigh-scattered light, further hampering optical methods which rely on molecular scattering of light. Thus, Laser Differential Interferometry may well be the dominant optical diagnostic tool in our planned Mach 6 facility as well.

References

[1] Steven P. Schneider, C. E. Haven, J. B. McGuire, Steven H. Collicott, and L. Randall. High-speed laminar-turbulent transition research in the Purdue quiet-flow Ludwieg tube. In *25th AIAA Fluid Dynamics Conference*, Colorado Springs, CO, June 1994. AIAA paper number AIAA-94-2504.

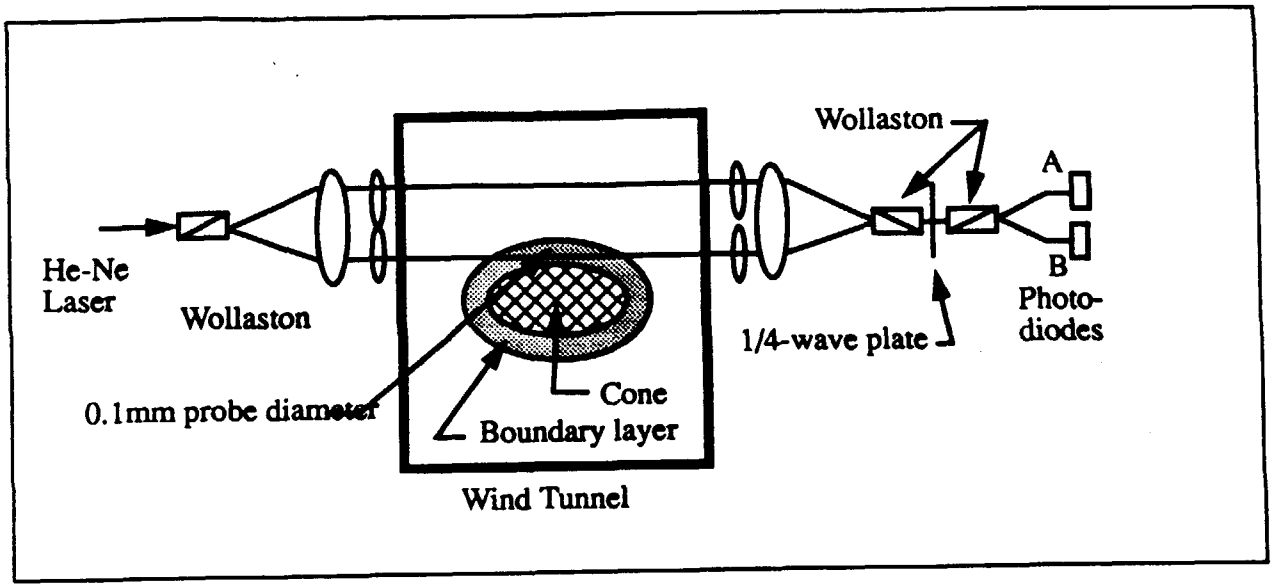

Figure 3: Layout of a basic Laser Differential Interferometer.

[2] G. Smeets. Interferometry. Technical Report Report CO 214/90, Institut Fracno-Allemand de Recherches de Saint-Louis, 1990.

[3] M. Azzazy, D. Modarress, and J. Trolinger. Feasibility study of optical boundary layer transition detection. Contractor Report NASA-CP-178109, NASA, 1986.

[4] J. E. O'Hare. A nonperturbing boundary-layer transition detector. Technical Report AEDC-TR-85-62, Arnold Engineering Development Center, November 1985.

[5] J.E. Harris and D.K. Blanchard. Computer program for solving laminar, transitional, or turbulent compressible boundary-layer equations for two-dimensional and axisymmetric flow. Technical Report NASA-TM-83207, NASA Technical Memorandum, 1982.

[6] L. M. Mack. Boundary layer linear stability theory. In *Special Course on Stability and Transition of Laminar Flow*. Advisory Group for Aerospace Research and Development, 1984. AGARD Report No. 709.

[7] C. Pruett and L. Ng. On the nonlinear stability of a high-speed, axisymmetric boundary layer. *Physics of Fluids A*, 3:2910–2926, 1991.

[8] K. Stetson and R. Kimmel. On hypersonic boundary-layer stability. Paper 92-0737, AIAA, 1992.

[9] A. Demetriades. Growth of disturbances in a laminar boundary layer at Mach 3. *Physics of Fluids A*, 1(2):312–317, 1989.

[10] James M. Kendall. Some comparisons of linear instability theory with experiment at supersonic and hypersonic speed. In M. Y. Hussaini and R.G. Voigt, editors, *Instability and Transition, Volume I*, pages 68–76. Springer-Verlag, 1990.

[11] A.J. Smits, H. Hayakawa, and K.C. Muck. Constant-temperature hot-wire anemometry practice in supersonic flows. *Experiments in Fluids*, 1:83–92, 1983.

[12] A.J. Smits and J.P. Dussauge. Hot-wire anemometry in supersonic flow. In *AGARDograph 315*, chapter 5. AGARD, 1989.

[13] D.A. Walker, W.F. Ng, and M.D. Walker. Experimental comparison of two hot-wire techniques in supersonic flow. *AIAA Journal*, 27:1074–1080, August 1989.

[14] Steven P. Schneider and Donald Coles. Experiments on single oblique laminar-instability waves in a boundary layer: Introduction, growth, and

transition. *The Physics of Fluids*, 6(3):1191–1203, March 1994.

[15] Steven P. Schneider. Improved methods for measuring laminar-turbulent intermittency in boundary layers, 1994. Submitted to *Experiments in Fluids*, January 1994.

[16] F. K. Owen. Transition experiments on a flat plate at subsonic and supersonic speeds. *AIAA Journal*, 8:518–523, 1970.

[17] M.J. Moen and S.P. Schneider. The effect of sensor size and substrate properties on the performance of flush-mounted hot-film sensors. In *Thermal Anemometry 1993, Proceedings of the Third ASME International Symposium on Thermal Anemometry*, pages 249–261. American Society of Mechanical Engineers, 1993. FED Volume 167.

[18] M.J. Moen and S.P. Schneider. The effect of sensor size on the performance of flush-mounted hot-film sensors. *Journal of Fluids Engineering*, 1994. Scheduled to appear in June 1994.

[19] S. P. Schneider and I. E. Beckwith. High speed boundary layer transition on a blunt nose flare with roughness. In *Proceedings of the 1991 ICASE/NASA Langley Workshop on Transition and Turbulence*, pages 18–27. Springer-Verlag, 1992.

[20] J.P. Clark, P.J. Magari, T.V. Jones, and J.E. LaGraff. Experimental studies of turbulent spot parameters using thin-film heat-transfer gauges. AIAA Paper 93-0544, AIAA, January 1993.

[21] J.D. Schmisseur, J.O. Young, and S.P. Schneider. Boundary-layer transition measurements on the sidewall of a quiet-flow ludwieg tube. Technical Report Paper 96-0852, AIAA, January 1996.

[22] P.P. Wegener and L.M. Mack. Condensation in supersonic and hypersonic wind tunnels. *Advances in Applied Mechanics*, 5:307–447, 1958.

[23] P.P. Wegener and G.D. Stein. Light-scattering experiments and theory of homogeneous nucleation in condensing supersonic flow. In *Proceedings of the 12th Combustion Institute*, pages 1183–1191, 1968.

[24] H. C. van de Hulst. *Light Scattering by Small Particles*. Wiley & Sons, New York, 1957.

[25] M. Volkan Ötügen, Kurt D. Annen, and Richard G. Seaholtz. Gas temperature measurements using a dual-line detection Rayleigh scattering technique. *AIAA Journal*, 31(11):2098–2104, November 1993.

[26] Rodney Loudon. *The quantum theory of light*. Oxford, Oxford, second edition, 1983.

[27] Zaidi B. Zakaria and Steven H. Collicott. Surface interference in Rayleigh scattering measurements near forebodies. *AIAA Journal*, 32(5):1098–1100, May 1994.

[28] Ronald J. Adrian. Particle-imaging techniques for experimental fluid mechanics. *Annual Review of Fluid Mechanics*, 23:261–304, 1991.

[29] J. F. Meyers and H. Komine. Doppler global velocimetry: A new way to look at velocity. In *ASME 4th International Conference on Laser Anemometry*, 1991.

[30] G. Smeets and A. George. Instantaneous laser Doppler velociemter using a fast wavelength tracking Michelosn interferometer. *Review of Scientific Instrumentation*, 49(11):1589–1596, Nov. 1978.

[31] Steinbichler Optotechnik GmbH., Neubeuem, Germany. *Laser Interference Velocimeter*, May 1994. Sales literature and communications.

[32] J. N. Forkey, W. R. Lembert, S. M. Bogdonoff, R. B. Miles, and G. Russell. Volumetric imaging of supersonic boundary layers using filtered Rayleigh scattering background suppression. In *AIAA 32nd Aerospace Sciences Meeting*, January 1994. AIAA-94-0491.

[33] Richard D. Keane and Ronald J. Adrian. Optimization of particle image velocimeters. *Measurement Science and Technology*, 1:97–110, 1990.

[34] Steven H. Collicott. Transition from particle image velocimetry to laser speckle velocimetry with increasing seeding density. In R. J. Adrian, editor, *Applications of Laser Techniques to Fluid Mechanics*, pages 181–194. Springer Verlag, 1993.

[35] TSI Inc. *Laser Velocimetry*. TSI sales literature.

[36] R. B. Miles, J. N. Forkey, and W. R. Lembert. Filtered Rayleigh scattering measurements in supersonic/hypersonic facilities. In *AIAA 17th Ground Testing Conference*, July 1992. AIAA-92-3894.

[37] A. Sugawara and S. Yip. Kinetic model analysis of light scattering by molecular gases. *Physics of Fluids*, 10(9):1911–1921, 1967.

[38] R. P. Sandoval and R. L. Armstrong. Rayleigh-Brillouin spectra in molecular nitrogen. *Physical Review A*, 13(2):752–757, 1976.

[39] I. Beckwith, F. Chen, and M. Malik. Transition research in low-disturbance high-speed wind tunnels. In *Laminar-Turbulent Transition*. Springer-Verlag, 1990. Proceedings of the IUTAM Symposium, Toulouse, France, September, 1989.

[40] I. Beckwith, T. Creel, F. Chen, and J. Kendall. Freestream noise and transition measurements on a cone in a Mach 3.5 pilot low-disturbance tunnel. Technical Report NASA-TP-2180, NASA Technical Paper, 1983.